Drug Design, Development and Therapy

Dovepress
open access to scientific and medical research

Open Access Full Text Article

ORIGINAL RESEARCH

Unveiling the Renoprotective Mechanisms of Schisandrin B in Ischemia-Reperfusion Injury Through Transcriptomic and Pharmacological Analysis

Changhong Xu[1,*], Yun Deng[1,*], Jiangwei Man[1,*], Huabin Wang[1], Tuanjie Che[2], Liyun Ding[3], Li Yang[1]

[1]Department of Urology, Institute of Urology, Gansu Province Clinical Research Center for Urinary System Disease, Lanzhou University Second Hospital, Lanzhou, Gansu, 730030, People's Republic of China; [2]Innovation Center of Functional Genomics and Molecular Diagnostics Technology of Gansu Province, Lanzhou, People's Republic of China; [3]School of Physical Science and Technology, Lanzhou University, Lanzhou, 730000, People's Republic of China

*These authors contributed equally to this work

Correspondence: Li Yang, Department of Urology, Institute of Urology, Gansu Province Clinical Research Center for Urinary System Disease, Lanzhou University Second Hospital, Lanzhou, Gansu, 730030, People's Republic of China, Email ery_yangli@lzu.edu.cn

Objective: This study investigates the targets, pathways, and mechanisms of Schisandrin B (Sch B) in alleviating renal ischemia-reperfusion injury (RIRI) using RNA sequencing and network pharmacology.

Methods: The effects of Sch B on RIRI were assessed using hematoxylin-eosin (HE) and periodic acid-Schiff (PAS) staining, along with measurements of blood creatinine and urea nitrogen (BUN). Differential gene expression in mouse models treated with RIRI and Sch B+RIRI was analyzed through RNA-Seq. Key processes, targets, and pathways were examined using network pharmacology techniques. The antioxidant capacity of Sch B was evaluated using assays for reactive oxygen species (ROS), mitochondrial superoxide, and JC-1 membrane potential. Molecular docking was employed to verify the interactions between key targets and Sch B, and the expression of these targets and pathway was confirmed using qRT-PCR, Western blot, and immunofluorescence.

Results: Sch B pre-treatment significantly reduced renal pathological damage, inflammatory response, and apoptosis in a mouse RIRI model. Pathological damage scores dropped from 4.33 ± 0.33 in the I/R group to 2.17 ± 0.17 and 1.5 ± 0.22 in Sch B-treated groups ($p < 0.01$). Creatinine and BUN levels were also reduced (from 144.6 ± 21.05 μmol/L and 53.51 ± 2.34 mg/dL to 50.44 ± 5.61 μmol/L and 17.18 ± 0.96 mg/dL, $p < 0.05$). Transcriptomic analysis identified four key targets (AKT1, ALB, ACE, CCL5) and the PI3K/AKT pathway. Experimental validation confirmed Sch B modulated these targets, reducing apoptosis and oxidative stress, and enhancing renal recovery.

Conclusion: Sch B reduces oxidative stress, inflammation, and apoptosis by modulating key targets such as AKT1, ALB, ACE, and CCL5, while activating the PI3K/AKT pathway, leading to improved renal recovery in RIRI.

Keywords: renal ischemia-reperfusion injury, schisandrin B, transcriptomics, network pharmacology, PI3K/AKT pathway

Introduction

Renal ischemia-reperfusion injury (RIRI) is widely prevalent in clinical practice, particularly in scenarios such as kidney transplantation, acute kidney damage, and cardiovascular surgeries. The onset of this pathological state involves multiple complex mechanisms, including oxidative stress, inflammatory responses, and cellular apoptosis,[1] which are pivotal factors. Oxidative stress is a central factor, arising from the overproduction of reactive oxygen species (ROS) during reperfusion. These ROS damage cellular components, including lipids, proteins, and DNA, which leads to mitochondrial dysfunction and amplifies cellular injury. In addition, ROS act as signaling molecules, triggering inflammatory responses

Received: 15 August 2024
Accepted: 18 September 2024
Published: 21 September 2024

and apoptosis.[2] Inflammation is another key driver of RIRI, characterized by the activation and infiltration of immune cells, such as neutrophils and macrophages, into the renal tissue. The ischemic insult prompts the release of pro-inflammatory cytokines, such as TNF-α, IL-6, and IL-1β, further promoting tissue damage and increasing oxidative stress. This creates a vicious cycle, where inflammation and oxidative stress exacerbate each other, ultimately contributing to renal dysfunction.[3] Furthermore, apoptosis plays a critical role in RIRI, particularly through mitochondrial and extrinsic pathways. The ischemic phase results in ATP depletion and cellular homeostasis disruption, while reperfusion triggers apoptotic signaling. Key regulators, including caspases and Bcl-2 family proteins, orchestrate the programmed cell death of renal tubular epithelial cells, leading to extensive cell loss and functional decline.[4] RIRI can lead to acute and chronic graft dysfunction in renal transplant recipients postoperatively, significantly impacting their prognosis.[2,5] Despite widespread recognition of this issue's importance, there is currently a lack of definitive and effective treatment strategies. Therefore, the search for new pharmacological treatments, especially those derived from natural sources, is particularly critical.

Schisandrin B (Sch B), a major active component derived from the traditional Chinese herbal medicine Schisandra chinensis, has been demonstrated to possess significant anti-inflammatory and antioxidative effects.[6,7] It also aids in enhancing the blood concentration of the immunosuppressant tacrolimus in liver and kidney transplant recipients, which helps to reduce postoperative complications and improve patient outcomes.[8,9] Existing research indicates that Sch B exerts protective effects in treating diseases such as diabetic cardiomyopathy[6] and acute lung injury[10] by alleviating inflammation, reducing oxidative stress, inhibiting apoptosis, and fibrosis. In studies of cardiac reperfusion injury, Sch B has been found to regulate mitochondrial glutathione status and membrane permeability.[11] Although its protective effects in various pathological models have been proven, the specific mechanisms and potential targets of Sch B in renal ischemia-reperfusion injury models require further investigation.

Transcriptomics, a technique that reveals variations in gene expression in specific physiological and pathological states by analyzing all RNA molecules expressed, lays the foundation for a deeper understanding of disease mechanisms and the identification of new biomarkers.[12] Network pharmacology, a modern pharmacological approach that integrates systems biology, computational biology, and pharmacoinformatics, reveals the multi-target mechanisms of drugs by establishing networks between drugs and biomolecules.[13] With the vast accumulation of biological data and advances in analytical technologies, network pharmacology has become an essential tool in drug development, providing scientific support for personalized medicine and precision treatment.

The ischemia-reperfusion model is a well-established and widely used approach for studying renal injury in experimental animals. In our study, we induced ischemia for 45 minutes, followed by 24 hours of reperfusion, a protocol that closely mirrors accepted clinical methodologies. This model is designed to replicate the conditions of renal ischemia-reperfusion injury seen in clinical settings. Various techniques, such as renal artery clamping, can be employed to induce ischemia; in our study, we chose the clamping method for its precision in controlling the ischemic duration. Uniquely, this study is the first to integrate transcriptomic analysis and network pharmacology to systematically explore the protective effects of Schisandrin B (Sch B) on renal ischemia-reperfusion injury and its underlying molecular mechanisms. The ultimate goal of this research is to provide new theoretical foundations and therapeutic strategies for renal protection, while also advancing the application of natural compounds in the treatment of kidney diseases.

Materials and Methods

Reagents and Antibodies

Sch B (S3600) was purchased from Selleck (Shanghai, China). Antibodies against phospho-AKT (Ser473) (p-AKT, 66444-1-Ig), AKT (60203-2-Ig), IL-6 (66,146-1-Ig), and goat anti-rabbit IgG-HRP secondary antibody (SA00001-2) were provided by Wuhan Proteintech Group, Inc. The CCK-8 assay kit (BS350B) was obtained from Biosharp (Hefei, China). DCFH-DA probe (MX4827) was purchased from Maokang (Shanghai, China). MitoSOX Red (S0061S), TUNEL apoptosis assay kit (C1089), and TMRE (C2001S) were sourced from Beyotime Biotechnology (Shanghai, China). Hematoxylin and eosin (H&E) staining kit (G1120) and PAS staining kit (G1281) were acquired from Solarbio (Beijing, China).

Ethical Compliance

All experimental protocols were approved by the Animal Ethics Committee of Lanzhou University Second Hospital under approval number D2023-413. We strictly followed the Guidelines for the Welfare and Ethics of Laboratory Animals (Ministry of Science and Technology of the People's Republic of China) for the management and care of the laboratory animals. Additionally, we adhered to the ARRIVE guidelines (https://arriveguidelines.org) for the reporting of in vivo experiments to ensure transparency and reproducibility.

Animal Experiments

In this study, male BALB/c mice provided by the Lanzhou Veterinary Research Institute were housed under controlled environmental conditions with sterile food and ad libitum access to water. The mice were randomly assigned to four experimental groups (n=6): Sham operation group (Sham), ischemia-reperfusion group (IR), ischemia-reperfusion with low-dose Sch B (20 mg*kg/day) group (IR+S20), and ischemia-reperfusion with high-dose Sch B (40 mg*kg/day) group (IR+S40).[6] In addition, each repeat was performed as a separate, independent experiment or observation. Mice in the Sch B treatment groups received the drug via oral gavage for 7 consecutive days, while the Sham and IR groups received an equivalent volume of corn oil via gavage. Subsequently, all mice, except those in the sham-operated group, underwent the procedure to establish the bilateral renal ischemia-reperfusion injury model. A 1.5–2 cm dorsal incision was made to expose both kidneys, and bilateral renal ischemia was induced by clamping the renal pedicles for 45 minutes, as indicated by a color change in the kidneys. After the ischemia period, the clamps were removed to allow reperfusion, and the incision was sutured. Postoperatively, mice were kept on a heating pad with analgesia provided. After 24 hours of reperfusion, the mice were euthanized, and the kidneys were harvested for analysis.[14]

HE Staining

Tissue samples were first fixed in 4% formaldehyde for 24 hours, followed by dehydration, clearing, and embedding (n=6). Sections were cut at a thickness of 4 microns. The sections underwent hematoxylin staining for 10 minutes and eosin staining for 1 minute, followed by dehydration in alcohol, clearing, and mounting. Finally, the slides were analyzed using an optical microscope.

PAS Staining

Periodic Acid-Schiff (PAS) staining is employed to detect polysaccharides and glycoproteins in tissue samples (n=6). After fixation and paraffin embedding, the samples underwent oxidation with 1% periodic acid, followed by staining with Schiff's reagent to form bright red complexes. The stained samples were then dehydrated and cleared to prepare slides for microscopic observation.

Blood Creatinine and Urea Nitrogen Measurement

Blood samples from all experimental mice were collected via retro-orbital puncture and immediately stored in sterile tubes at 4°C. Serum levels of creatinine and urea nitrogen were measured using an automated biochemical analyzer (Beckman Coulter, AU480, USA)(n=6). Prior to biochemical analysis, all blood samples were centrifuged to separate the serum or supernatant. Creatinine levels were determined using the modified Jaffé method, which is based on the reaction of creatinine with picric acid in an alkaline environment to form a red complex. The absorbance of this complex, which is proportional to the creatinine concentration, was measured at a wavelength of 495 nanometers. Urea nitrogen levels were determined using the urease method, in which urea is decomposed into carbon dioxide and ammonia by urease. The ammonia subsequently reacts with a specific reagent to form a colored product measurable at a wavelength of 340 nanometers.

Tissue Immunofluorescence

Immunofluorescence staining techniques were employed to localize and quantify p-AKT and IL-6 proteins in tissue sections (n=6). Initially, antigen retrieval was performed in citrate buffer, followed by blocking with BSA to reduce background interference. Subsequently, the sections were incubated overnight with primary antibodies targeting p-AKT

and IL-6. Afterward, fluorescently labeled secondary antibodies and DAPI staining were applied to mark the cell nuclei. A fluorescence microscope was used to capture and analyze the images of the samples, allowing for precise detection and analysis of the expression and localization of these proteins.

Transcriptomic Sequencing

RNA was extracted from renal tissue samples (n=5 per group), stored at −80°C, using Trizol reagent (Invitrogen). RNA quality and quantity were assessed using a NanoDrop spectrophotometer and Bioanalyzer to ensure RNA integrity (RIN > 7.0). The sequencing library was constructed with the Illumina TruSeq RNA Sample Preparation Kit (Illumina, San Diego, CA, USA) following the manufacturer's instructions, and samples were sequenced on the Illumina HiSeq 4000 platform to generate 150 bp paired-end reads. Quality control of raw sequencing data was performed using FastQC and Trimmomatic to remove low-quality reads and adapter sequences. Reads were aligned to the human reference genome (GRCh38) using the HISAT2 tool, allowing for mismatches and splice junctions. Transcript abundance was quantified, and differential expression analysis was conducted using DESeq2, with an adjusted P-value < 0.05 (Benjamini-Hochberg correction) and an absolute log2FoldChange > 1. Functional enrichment analysis of differentially expressed genes was performed using DAVID and Gene Ontology (GO) annotations to explore the biological processes involved in renal ischemia-reperfusion injury.

RNA Extraction and Quantitative Real-Time PCR (qRT-PCR)

Total RNA was isolated from kidney samples using Trizol reagent (n=6). The first-strand cDNA synthesis was carried out using 2 μg of RNA as the template and the Evo M-MLV RT Kit. For quantitative real-time PCR (qRT-PCR), the CFX96 Real-Time PCR Detection System and SYBR Green Premix were utilized, with β-actin employed as the internal control to standardize gene expression levels. The specific PCR primers and genes examined are listed in Table 1. The PCR conditions included an initial denaturation at 95°C for 30 seconds, followed by 50 cycles consisting of a 10-second denaturation at 95°C and a 30-second annealing phase at 60°C.

Identification of Sch B and RIRI Targets

To identify potential targets of Sch B, we utilized four online databases: TCMSP (https://tcmspw.com/), CTD, HERB, and Swiss Target Prediction for preliminary target identification, followed by deduplication of results. For RIRI targets, we employed the DisGeNET (https://www.disgenet.org/) and GeneCards (https://www.genecards.org/) databases, filtering for entries with scores higher than 2.5. We integrated these targets and converted the data to specific protein IDs and corresponding gene names using the UniProt database (https://www.uniprot.org/).

GO and KEGG Enrichment Analysis

Using R 4.3.2 software, we performed GO (Gene Ontology) and KEGG (Kyoto Encyclopedia of Genes and Genomes) enrichment analysis on transcriptomic differentially expressed genes (TDEGs), intersecting genes related to Sch B and renal IRI. We prioritized the top 30 KEGG pathways and top 10 GO terms related to Sch B's role in combating RIRI based on adjusted P-values (P<0.05). The results were visualized in the form of bar graphs using appropriate R 4.3.2 packages.

Table 1 Design of Primers for the Genes Involved in the Experiment

Gene	Species	Forward	Reverse
AKT1	Mus musculus	CCGCCTGATCAAGTTCTCCT	GATGATCCATGCGGGGCTT
ALB	Mus musculus	CAGCGGAGCAACTGAAGACT	GGTTTGGACCCTCAGTCGAG
ACE	Mus musculus	CCACTGACAGAATGGCTCGT	TGGGTGTAGTACCGGTGTTTG
CCL5	Mus musculus	ATATGGCTCGGACACCACTC	ACTTGGCGGTTCCTTCGAG

Network Construction for Sch B Regulation of RIRI

The intersecting genes were uploaded to the STRING database (https://string-db.org) with parameters set to "Homo sapiens" and a confidence threshold of 0.96 to generate a protein-protein interaction (PPI) network. This network was then refined using Cytoscape 3.9.1, employing the cytoNCA plugin to pinpoint key hub genes. The results were subsequently incorporated into a comprehensive "Sch B-Gene-Pathway-RIRI" PPI network, which was informed by GO and KEGG enrichment analyses. This integrative approach facilitates a deeper understanding of the molecular interactions and pathways modulated by Sch B in renal ischemia-reperfusion injury, potentially identifying novel therapeutic targets or mechanisms.

Molecular Docking

Ligand structures were obtained in two-dimensional format from the PubChem database, converted to three-dimensional models using ChemBio3D Ultra 14.0.0, and subjected to energy minimization using the MMFF94 force field. Core target proteins associated with identified genes (eg, AKT1, ALB, ACE, CCL5) were retrieved from the UniProt database, and their 3D structures were downloaded from the RCSB Protein Data Bank (PDB). Receptor proteins were prepared using PyMol 2.6, with water molecules and co-crystallized ligands removed, and hydrogen atoms were added using AutoDockTools 1.5.6 to optimize the receptor conformation. The active sites were defined based on known binding pockets or predicted using CASTp. Molecular docking was performed using AutoDock Vina 1.2.2, with a grid box centered on the binding pocket. Docking results were evaluated based on binding affinity, with the lowest energy conformation selected for further analysis. Key interactions, including hydrogen bonds, hydrophobic interactions, and electrostatic forces, were visualized and analyzed using PyMol to confirm the stability of ligand-receptor interactions.

Cell Culture

The HK-2 cell line, which was purchased from Servicebio (Cat number: STCC10303P), is a human renal epithelial cell line that resembles the proximal tubular cells of the kidney. The DMEM/F-12 medium (Gibco, C11330500BT, USA) for culturing the HK-2 Cell Line was enriched with 10% fetal bovine serum, 100 U/mL penicillin, and 100 μg/mL streptomycin. The cells were incubated at 37°C under conditions of 5% CO_2 and 21% O_2, maintaining a pH of 7.4.

Establishment and Pre-Treatment of Hypoxia/Reoxygenation (HR) Model

To replicate in vivo RIRI, HK-2 cells were subjected to hypoxia-reoxygenation (HR) treatment in vitro. This process began with exposing the cells to a hypoxic atmosphere of 94% N_2, 5% CO_2, and 1% O_2 in a tri-gas incubator, using a serum-free and glucose-free medium for 12 hours. Reoxygenation was then performed under standard conditions (5% CO_2 and 21% O_2) for 2 hours, switching to DMEM/F-12 medium containing 10% serum. In the Sch B pre-treatment group, HK-2 cells were pre-treated with 20 μmol/L Sch B 12 hours before hypoxia, followed by the HR procedure.

Measurement of Intracellular ROS Levels

Intracellular reactive oxygen species (ROS) levels were assessed using the DCFH-DA probe (MKBIO, MX4802-50MG, China). The cells were incubated with a 5 μmol/L DCFH-DA solution at 37°C for 30 minutes. Following incubation, fluorescence was observed and captured using a fluorescence microscope, with an excitation wavelength of 488 nm and an emission wavelength of 525 nm. The average fluorescence intensity of DCFH-DA was measured and quantified using ImageJ software (n=6).

Detection of Mitochondrial Superoxides

To detect the production of reactive oxygen species (ROS) in mitochondria, the MitoSOX Red reagent kit (Beyotime, S0061S, China) was used. Cells grown in 6-well plates had their culture medium removed and were rinsed once with phosphate-buffered saline (PBS) to eliminate any residual media and metabolic by-products that might interfere with the staining process. Subsequently, 1 mL of MitoSOX Red staining solution was added to each well, followed by a 30-minute incubation at 37°C. After incubation, the cells were washed twice with PBS. Then, 2 mL of PBS was added to

each well, and mitochondrial superoxides were visualized using a Zeiss LSM880 confocal microscope with the CY3 channel. The fluorescence intensity of mitochondrial superoxides was analyzed and quantified using ImageJ software (n=6).

Measurement of Mitochondrial Membrane Potential

The JC-1 Mitochondrial Membrane Potential Assay Kit was employed to measure alterations in the mitochondrial membrane potential of HK-2 cells following hypoxia/reoxygenation treatment. After removing the culture medium, the cells were washed once with PBS. Subsequently, 1 mL of JC-1 working solution was added to each dish, and the cells were incubated for 30 minutes to allow the dye to accumulate in the mitochondria. The variations in mitochondrial membrane potential were visualized using a Zeiss LSM880 confocal microscope equipped with a 60×1.3 NA oil immersion lens. Fluorescence signals were detected through the A546 and A488 channels. The acquired images were analyzed and quantified with ImageJ software to assess the mitochondrial membrane potential changes (n=6).

Measurement of Cell Apoptosis

The apoptosis in HK-2 cells was evaluated using a TUNEL Apoptosis Assay Kit (Beyotime, C1090, China). Cells (3x10^6) were plated on 25mm coverslips coated with poly-L-lysine and allowed to culture for 24 hours prior to HR treatment. Both control and HR-exposed cells were fixed in 4% paraformaldehyde and permeabilized with 0.3% Triton X-100 for 10 minutes. The cells were then incubated with the TUNEL reaction mixture at 37°C in the dark for 60 minutes. Following incubation, the cells were rinsed twice with PBS, stained with DAPI in the dark for 10 minutes, washed again twice with PBS, and subsequently observed under a fluorescence microscope using the Cy3 channel (n=6).

Western Blotting

Proteins were isolated from HK-2 cells using RIPA (Solarbio, R0010, China) buffer supplemented with protease and phosphatase inhibitors. The protein concentrations were determined with a BCA assay kit. Samples containing 30 μg of protein were separated by SDS-PAGE on 10% or 15% gels, depending on protein size, and subsequently transferred to PVDF membranes (Beyotime, FFP20, China). The membranes were blocked with 5% non-fat milk in TBST for 1 hour, followed by overnight incubation with primary antibodies. After washing with TBST, the membranes were incubated with secondary antibodies at room temperature for 1 hour. Detection was performed using an ECL system, and the protein band intensities were quantified with ImageJ software.

Statistical Analysis

Data were expressed as mean ± standard deviation. Comparisons between groups were conducted using one-way ANOVA followed by Dunnett's multiple comparison test. Statistical analysis was performed using GraphPad Prism 10.1 software, with a p-value of less than 0.05 considered statistically significant.

Results

Sch B Pre-treatment Reduces Pathological Damage, Inflammatory Response, and Apoptosis in Mouse Kidneys Post-Ischemia Reperfusion

To explore the effects of Sch B on RIRI, we employed a series of techniques including HE, PAS staining, creatinine and urea nitrogen measurements, immunofluorescence, and TUNEL staining to validate the action of Sch B. As shown in Figure 1A, kidneys from mice subjected to IR modeling exhibited significant pathological damage, including thinning and necrosis of renal tubular epithelial cells, loss of the brush border, and formation of tubular casts, accompanied by inflammatory cell infiltration. The extent of these damages was reduced in a concentration-dependent manner with Sch B pre-treatment. Figure 1B illustrates the pathological damage scores across the Sham, IR, IR+S10, and IR+S20 groups (Sham: 0.5 ± 0.22, IR: 4.33 ± 0.33, IR+S10: 2.17 ± 0.17, IR+S20: 1.5 ± 0.22, $p < 0.01$ for both comparisons with the IR group), confirming a reduction in damage severity with Sch B treatment. In terms of renal function, plasma creatinine and urea nitrogen (BUN) levels were significantly elevated in the IR group (Creatinine: 144.6 ± 21.05 μmol/L, BUN: 53.51 ±

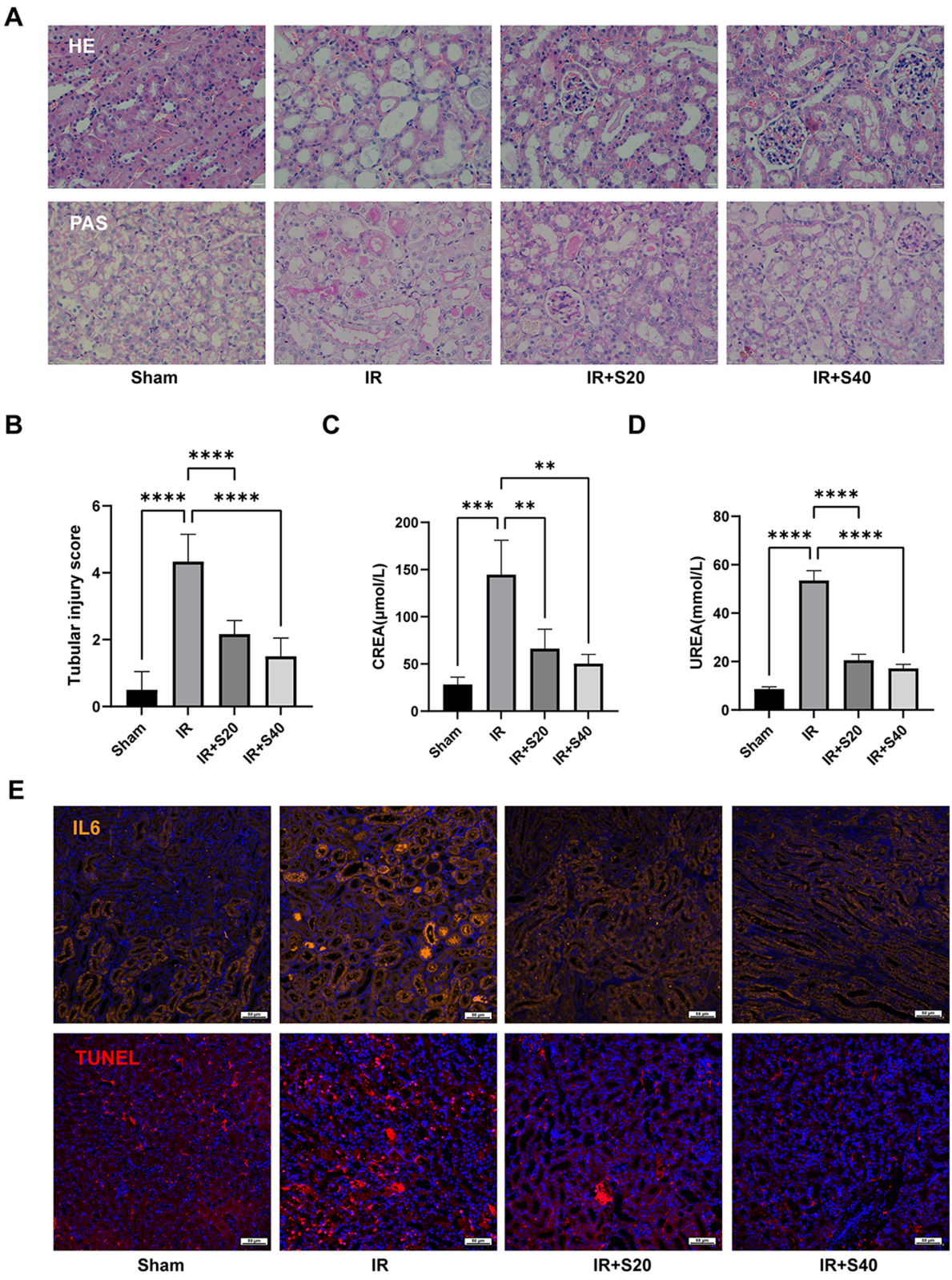

Figure 1 Schisandrin B pretreatment reduces pathological damage, inflammatory response, and apoptosis levels in mouse kidneys after ischemia-reperfusion (IR). (**A**) H&E and PAS staining of kidney tissues. (**B**) Pathological damage scores across Sham, IR, IR+S10, and IR+S20 groups (n = 6). (**C**) Plasma creatinine levels (n = 6). (**D**) Plasma urea nitrogen levels (n = 6). (**E**) IL-6 expression and TUNEL-positive cell analysis (n = 6). Data are presented as mean ± SEM; significance is denoted as *p < 0.05, **p < 0.01, ***p < 0.001, ****p < 0.0001. The analysis was performed using ImageJ (n = 6).

2.34 mg/dL) compared to the Sham group (Creatinine: 28.26 ± 4.53 μmol/L, BUN: 8.67 ± 0.51 mg/dL, $p < 0.001$ for both). In the IR+S10 and IR+S20 groups, these levels significantly decreased, indicating a recovery of renal function (Creatinine in IR+S10: 66.29 ± 11.86 μmol/L, IR+S20: 50.44 ± 5.61 μmol/L; BUN in IR+S10: 20.55 ± 1.42 mg/dL, IR +S20: 17.18 ± 0.96 mg/dL, $p < 0.05$ for both groups compared to the IR group). Post-IR, the expression levels of IL-6 in the kidneys were significantly elevated, indicating enhanced inflammatory response. Concurrently, the number of TUNEL-positive cells increased significantly, indicating heightened apoptosis. In the IR+S10 and IR+S20 groups, both IL-6 expression levels and the number of TUNEL-positive cells showed a dose-dependent reduction (See Figure 1E), indicating that Sch B pre-treatment reduced renal inflammation and apoptosis levels.

Transcriptomic and Network Pharmacological Analysis of Sch B Treatment on RIRI

Transcriptomic sequencing was performed on the kidneys of mice from the IR+S20 and IR groups, and analysis of the transcriptomic data matrix identified 1842 differentially expressed genes (DEGs). Heatmaps and volcano plots in Figure 2A and B display the distribution of these DEGs. A total of 442 potential targets of Sch B were identified from TCMSP, CTD, HERB, and Swiss Target Prediction after deduplication. Additionally, 2416 potential targets for RIRI were identified and deduplicated from DisGeNET and GeneCards. As shown in Figure 2C, a Venn diagram constructed using online platforms revealed 22 intersecting targets among DEGs, Sch B, and RIRI. Figure 2D illustrates a protein-protein interaction (PPI) map between the 22 intersecting targets.

GO enrichment of the 22 intersecting targets resulted in 832 biological processes (BPs), with the top ten including positive regulation of kinase activity, response to oxygen levels, and protein autophosphorylation (Figure 2E). A total of 21 cellular components (CCs) were enriched, with the top ten including blood microparticles, collagen-containing extracellular matrix, and peroxisomes. Additionally, 64 molecular functions were enriched, with the top ten including oxidoreductase activity acting on CH-NH2 group donors with oxygen as the acceptor. KEGG pathway enrichment results

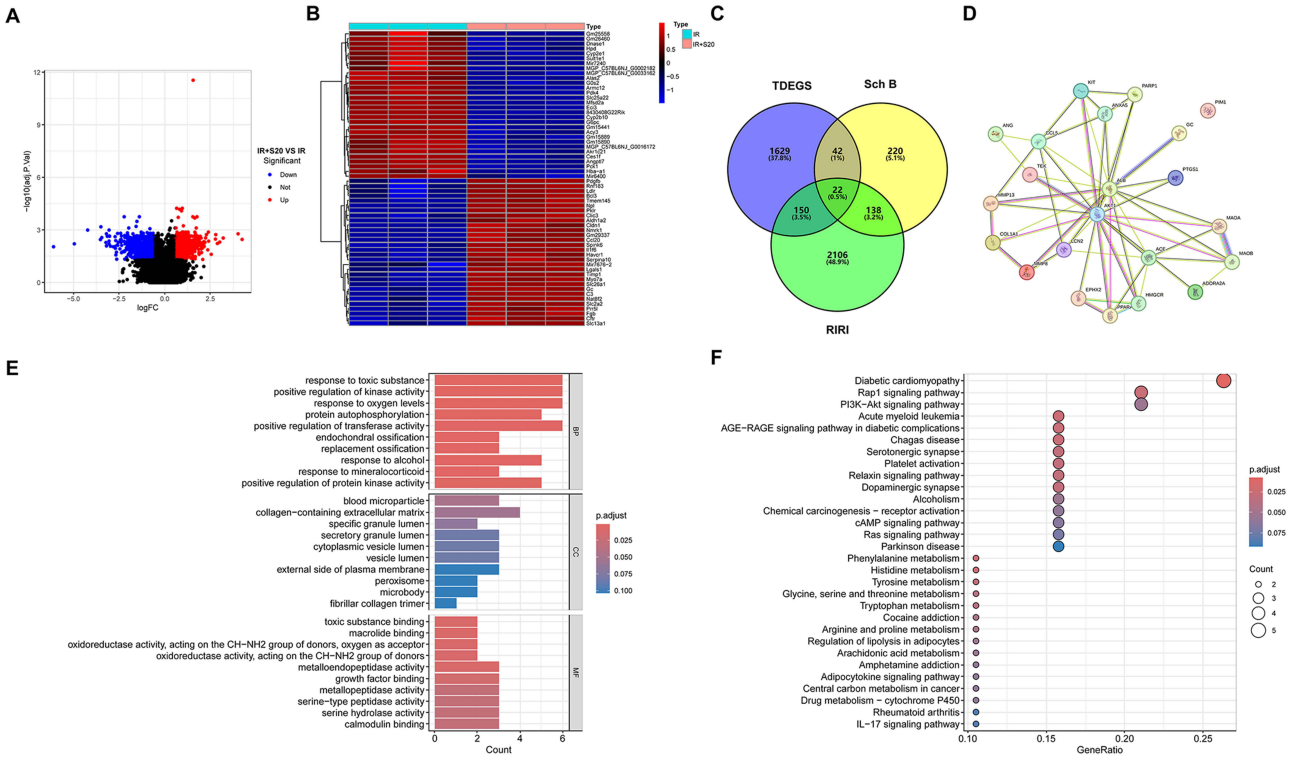

Figure 2 Transcriptomic and Network Pharmacology Analysis of Schisandrin B Treatment for Renal Ischemia-Reperfusion Injury (RIRI). (**A**) Volcano plot illustrating DEGs. (**B**) Heatmap showing differential gene expression. (**C**) Venn diagram depicting intersecting targets. (**D**) Protein-Protein Interaction (PPI) Maps. (**E**) GO enrichment for cellular components (CC). (**F**) KEGG pathway enrichment analysis.

depicted in Figure 2F highlighted 30 potential pathways, with the most significantly enriched including the PI3K-Akt signaling pathway and the Rap1 signaling pathway.

Selection of Key Targets and Construction of a Drug-Target-Pathway-Function Enrichment-Disease Network

The PPI network identified 22 nodes and 110 edges, ultimately pinpointing four key targets: AKT1, ALB, ACE, and CCL5, as shown in Figure 3A. Nodes filled in red indicate strong interactions within the network, highlighting the significant roles of these targets among the intersecting targets. Additionally, the targets, pathways, and function enrichments of Sch B and RIRI were visualized in the form of a drug-target-pathway-function enrichment-disease network, as seen in Figure 3B.

Molecular Docking of Sch B with Key Targets

As shown in Figure 4, molecular docking of Sch B with four key targets (AKT1, ALB, ACE, and CCL5) revealed strong binding affinities. Sch B exhibited the highest affinity for AKT1 with a binding energy of −8.79 kcal/mol, followed by ALB at −7.962 kcal/mol and ACE at −7.564 kcal/mol. The interaction with CCL5 showed a lower binding affinity of −5.39 kcal/mol. In all cases, Sch B formed two or more hydrogen bonds, with RMSD values of 0.00 Å in the best docking modes, indicating stable interactions.

Sch B Reduces Oxidative Stress and Apoptosis in HK-2 Cells Post-HR

Based on the results from transcriptomic and network pharmacological analysis, we validated the antioxidative capability of Sch B in HK-2 cells post-HR. Figure 5A shows that DCFH-DA fluorescence indicated elevated ROS levels in HK-2 cells post-HR, suggesting increased intracellular oxidative stress, while Sch B pre-treatment reduced this manifestation. The detection of mitochondrial superoxides suggested that levels were elevated in the HR group, while Sch B treatment reduced these levels, indicating decreased oxidative stress (Figure 5B). Additionally, Figure 5C shows an increase in TUNEL-positive cells in the HR group, indicating higher levels of DNA fragmentation and increased apoptosis. The number of TUNEL-positive cells was reduced in the HR+S20 group compared to the HR group, suggesting decreased apoptosis levels. Figure 5D shows that post-HR model establishment, the HR group had reduced levels of JC-1 aggregates and increased levels of JC-1 monomers, indicating loss of mitochondrial membrane potential. Pre-treatment with Sch B ameliorated this trend.

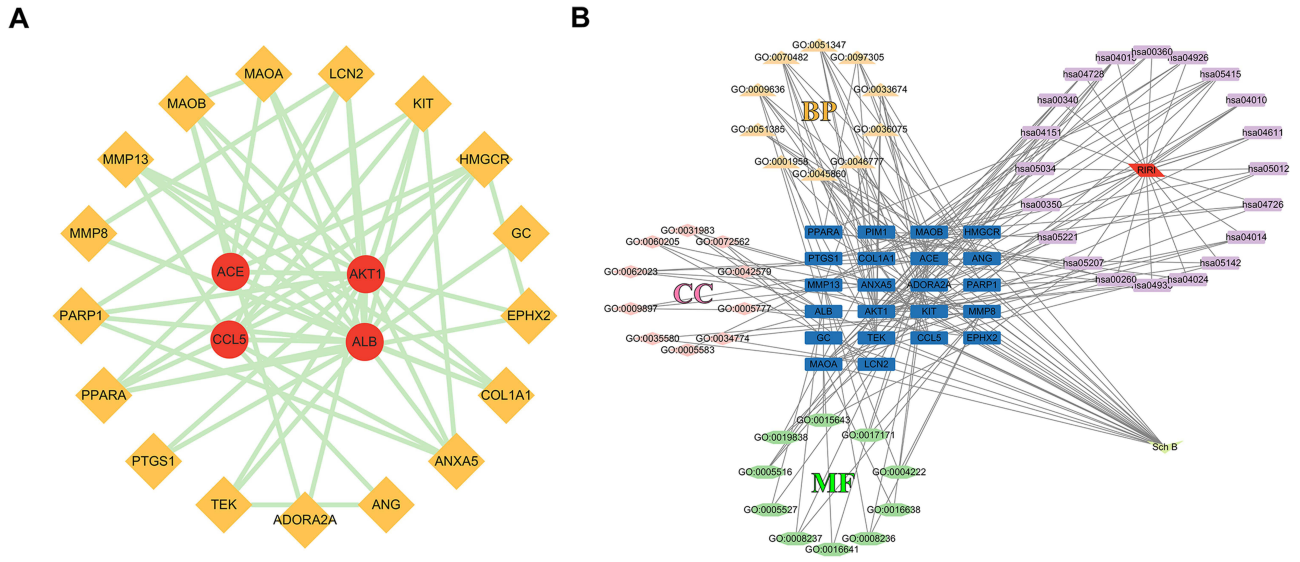

Figure 3 Selection of Key Targets and Establishment of Drug-Target-Pathway-Functional Enrichment-Disease Networks. (**A**) Protein-protein interaction (PPI) network highlighting key targets. (**B**) Integrated network of drug-target-pathway-function-disease associations.

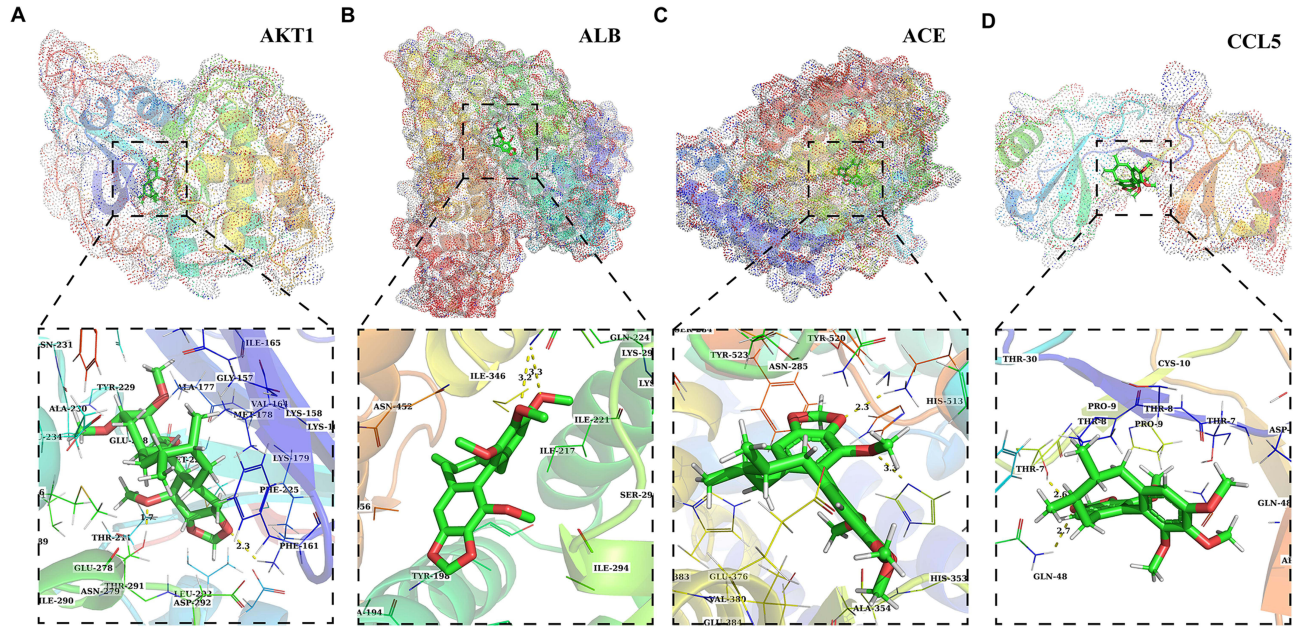

Figure 4 Molecular Docking of Schisandrin B with Key Targets. (**A**) Molecular docking of Sch B with AKT1. (**B**) Molecular docking of Sch B with ALB. (**C**) Molecular docking of Sch B with ACE. (**D**) Molecular docking of Sch B with CCL5.

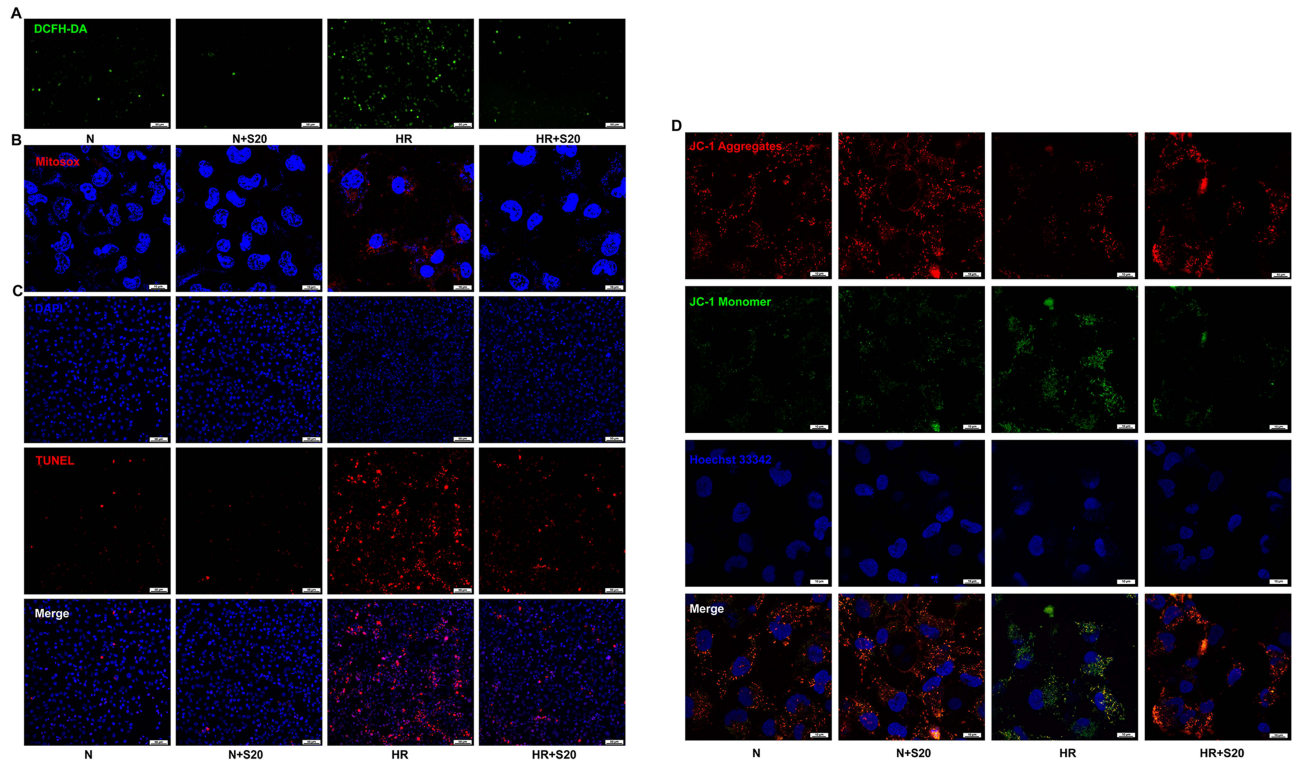

Figure 5 Schisandrin B reduces oxidative stress and apoptosis levels in HK-2 cells after hypoxia-reoxygenation (HR). (**A**) Detection of ROS using DCFH-DA fluorescence (n = 6). (**B**) MitoSOX staining for mitochondrial superoxide levels (n = 6). (**C**) TUNEL assay for apoptotic cell detection (n = 6). (**D**) JC-1 assay for mitochondrial membrane potential analysis (n = 6).

Sch B Regulates RIRI Through Control of AKT1, ALB, ACE, CCL5, and the PI3K/AKT Pathway

To verify the consistency of the predicted potential targets and key pathways of Sch B in treating RIRI, we conducted validations using renal tissues from mice with the IRI model and HK-2 cell lines subjected to the hypoxia-reoxygenation

(HR) model. As shown in Figures 6A–D, the mRNA expression levels of AKT1, ALB, and CCL5 were significantly decreased in the kidneys of the I/R group compared to the sham group. Specifically, AKT1 expression was reduced by 54.7% (from 1.000 to 0.4533 ± 0.09757, p<0.001), ALB by 48.4% (from 1.000 to 0.5163 ± 0.06788, p<0.001), and CCL5 by 67.3% (from 1.000 to 0.3270 ± 0.03372, p<0.001). However, in the Sch B pre-treatment groups, these markers showed varying degrees of recovery. In the IR + S10 group, AKT1 increased to 0.6773 ± 0.09510 (p<0.05), ALB to 0.6483 ± 0.05378 (p<0.05), and CCL5 to 0.6657 ± 0.05750 (p<0.05). In the IR + S20 group, AKT1 increased to 0.8433 ± 0.07396 (p<0.01), ALB to 0.7753 ± 0.1128 (p<0.01), and CCL5 to 0.9217 ± 0.06982 (p<0.01). In contrast, the expression pattern of ACE was opposite to that of the other three molecules. In the I/R group, ACE mRNA levels were elevated by 106.7% (from 1.000 to 2.067 ± 0.08556, p<0.001), but were reduced in the Sch B pre-treatment groups to 1.685 ± 0.07826 (p<0.05) in the IR + S10 group and 1.536 ± 0.04140 (p<0.05) in the IR + S20 group. Phosphorylation of AKT protein largely represents the activation of the PI3K/AKT pathway. Figure 6E, displaying results from immunofluorescence slices of animal tissues, indicates that the phosphorylation level of AKT protein was significantly reduced in the IR group. With graded application of Sch B, the phosphorylation levels gradually increased. This phenomenon was also observed in the HK-2 cell line post-HR through Western blot analysis: Sch B was able to restore the decrease in intracellular AKT phosphorylation levels brought about by

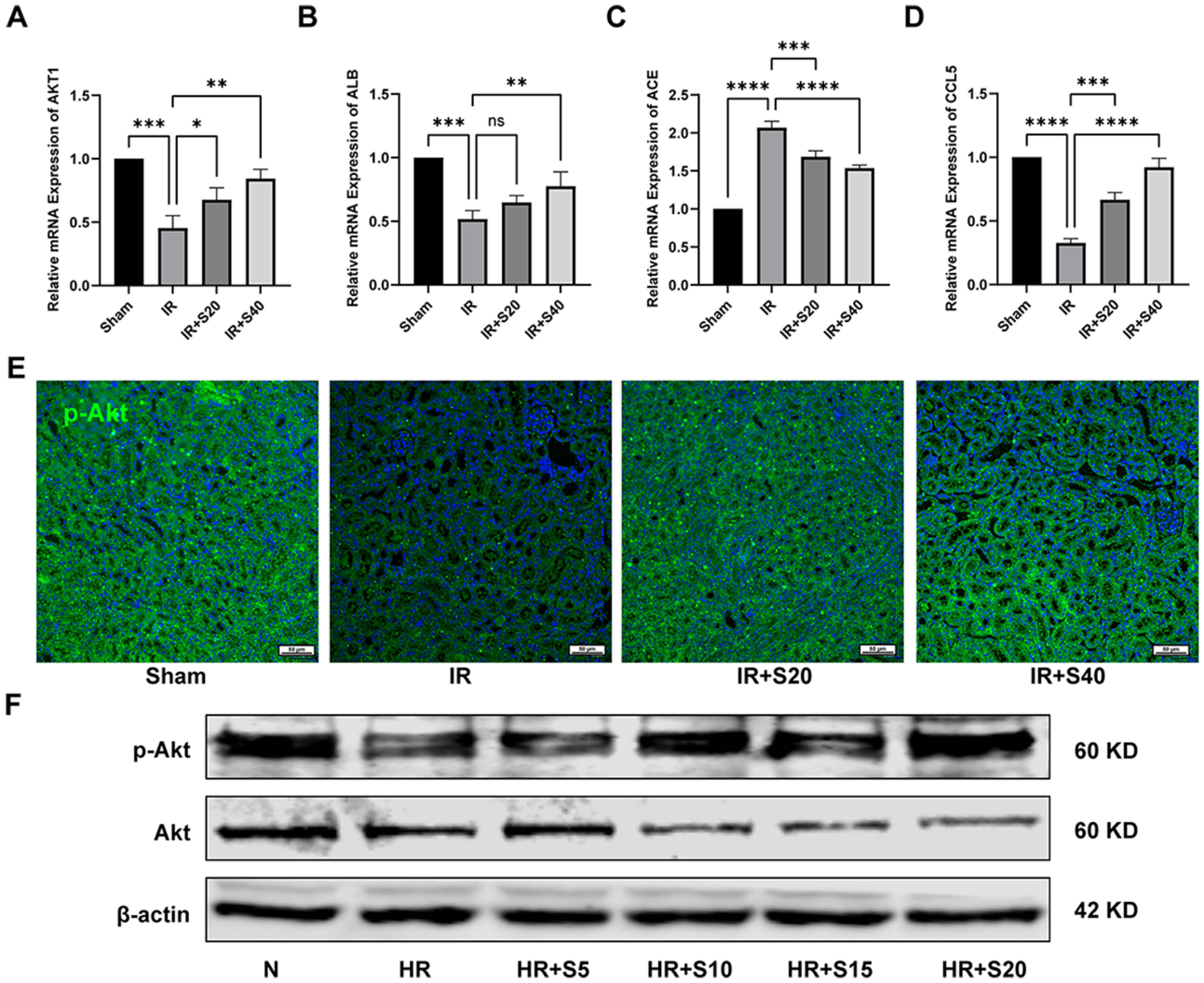

Figure 6 Schisandrin B can regulate renal ischemia-reperfusion injury (RIRI) through modulation of AKT1, ALB, ACE, CCL5, and the PI3K/AKT pathway. (**A**) mRNA expression of AKT1 (n = 6). (**B**) mRNA expression of ALB (n = 6). (**C**) mRNA expression of CCL5 (n = 6). (**D**) mRNA expression of ACE (n = 6). (**E**) Immunofluorescence analysis of p-AKT in kidney tissues (n = 6). (**F**) Western blot analysis of p-AKT in HK-2 cells. Data are presented as mean ± SEM; significance is denoted as *p < 0.05, **p < 0.01, ***p < 0.001, ****p < 0.0001. The analysis was performed using ImageJ (n = 6).

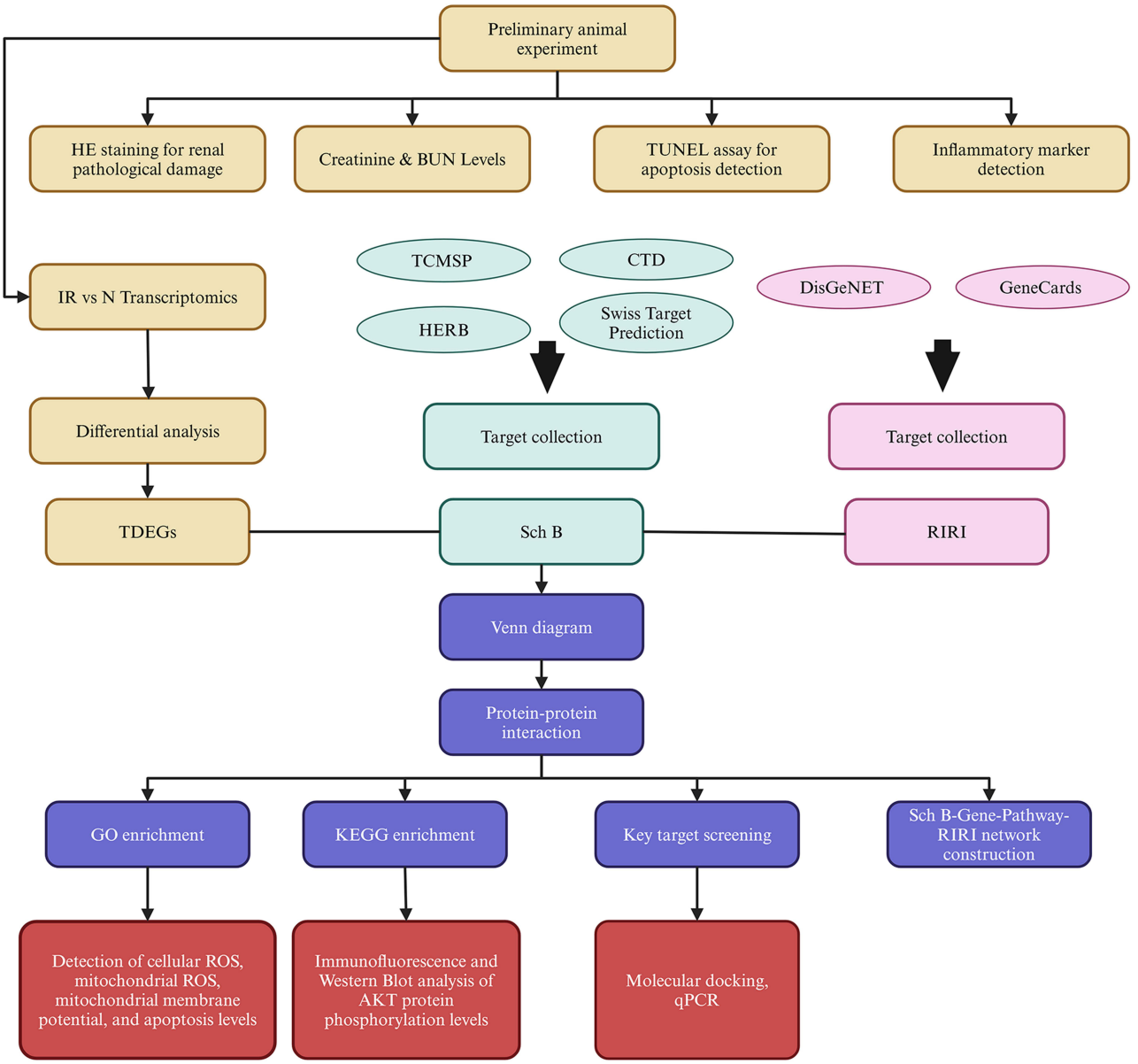

Figure 7 A flowchart illustrating the exploration of key targets and mechanisms of Schisandrin B in protecting against renal ischemia-reperfusion injury through transcriptomics and network pharmacology.

HR (Figure 6F). These results confirm that Sch B indeed regulates AKT1, ALB, ACE, and CCL5 in RIRI, and participates in the activation of the PI3K/AKT pathway during the IRI process. Figure 7 presents a schematic diagram illustrating the workflow of investigating the key targets and mechanisms by which Sch B protects the kidneys from ischemia-reperfusion injury through transcriptomics and network pharmacology studies.

Discussion

Previous studies have demonstrated the protective role of Sch B in various organ ischemia-reperfusion injuries.[11,15] This study is the first to explore the potential targets and pathways of Sch B against RIRI using transcriptomics combined with network pharmacology, and to further verify the analytical results through in vivo and in vitro experiments. This research presents the following findings: (i) In vivo experiments showed that Sch B pre-treatment alleviated pathological damage and inflammatory responses in RIRI, partially restoring renal function; (ii) Transcriptomic sequencing and network pharmacological enrichment analysis revealed that Sch B primarily interacts with protein phosphorylation and redox

reactions; (iii) Transcriptomic and network pharmacological screening identified four key targets of Sch B action: AKT1, ALB, ACE, CCL5, and a key pathway: the PI3K/AKT pathway; (iv) Sch B reduced oxidative stress damage in HK-2 cells post-HR; (v) Further in vivo and in vitro experiments confirmed the expression of key targets and pathways. These results highlight Sch B's renal protective and therapeutic effects and its molecular mechanisms in RIRI.

The RIRI model is one of the most extensively used experimental approaches for studying AKI. Regarding the duration of ischemia and reperfusion in mouse models of RIRI, there is considerable variation across studies. However, elevated levels of injury markers such as serum creatinine and BUN have consistently been observed. In a study on exosomal miR-125b-5p's role in alleviating RIRI, it was noted that clamping the renal pedicles for 30 minutes in mice induced bilateral I/R injury.[16] In contrast, Carlström et al[17] set the clamping time for bilateral renal pedicles at 20 minutes in their study. A more common and widely used model involves clamping the bilateral renal pedicles for 45 minutes, followed by 24 hours of reperfusion, as mentioned in the methodologies of Chu et al[14] and Hu et al.[18] Additionally, Kar et al,[19,20] in their study on the effects and mechanisms of curcumin and boric acid on RIRI, also demonstrated that 45 minutes of ischemia followed by 24 hours of reperfusion is an optimal application time for this model. Consistent with the model's importance, we adopted a well-established ischemia duration of 45 minutes followed by reperfusion for 24 hours. This protocol allowed us to simulate clinically relevant scenarios of ischemic damage and post-reperfusion inflammation.

Sch B's protective effects on various organ ischemia-reperfusion injuries include anti-apoptosis, anti-oxidative stress, anti-mitochondrial dysfunction, and anti-inflammatory responses. Zhang et al[21] found that Sch B pre-treatment could attenuate the expression levels of ER stress-related proteins such as CHOP, ATF6, and PERK, thereby reducing ER stress-associated apoptotic responses and providing protection against cardiac IRI. Our study indicates that Sch B reduces renal pathological damage, lowers plasma creatinine and urea nitrogen levels, and decreases levels of the inflammatory cytokine IL-6 and apoptosis. Zhu et al[22] showed that Sch B treatment in rats alleviated pathological damage in the lower limbs, with reduced expression of TNF-α and IL-1β, thereby lessening the severity of the inflammatory response.

Transcriptomic sequencing and network pharmacology comprehensively collect and analyze relevant targets, with combined application enhancing the accuracy and practicality of predictions. Based on transcriptomic and network pharmacological enrichment analysis, we predicted that Sch B mainly participates in redox reactions and protein autophosphorylation. During the IR process, mitochondria are the primary site for ROS production.[23] Studies have shown that excessive production of reactive oxygen species can increase renal tubular epithelial cell IR injury. Mitochondrial ROS can decrease mitochondrial membrane potential, inducing pro-apoptotic factors such as Cytochrome C to leak from the mitochondria into the cytosol, activating caspase-3 and promoting mitochondrial apoptosis. The damage to mitochondrial function, in turn, promotes ROS production, further exacerbating mitochondrial damage. Therefore, in our in vitro experiments, we measured the levels of intracellular reactive oxygen and mitochondrial superoxides to assess the cellular oxidative stress level. Results showed that Sch B reduced oxidative stress damage in HK-2 cells during HR. Consistent with our findings, Sch B, as a traditional antioxidant, effectively reduced liver damage caused by carbon tetrachloride[23] and oxidative stress imbalance induced by cisplatin.[24]

In addition, based on transcriptomics and network pharmacology, we identified four key targets for Sch B against RIRI: AKT1, ALB, ACE, and CCL5. AKT1 is a molecular subtype of the AKT protein, which regulates various cellular functions, including proliferation, survival, metabolism, and angiogenesis, in both normal and malignant cells. Previous studies have demonstrated that enhanced expression of mitochondrial AKT1 in renal tubular epithelial cells can protect the kidney from IRI and reduce the progression from AKI to renal fibrosis.[25] Our study suggests that the protective effects of Sch B against RIRI are related to the expression of AKT1. We observed upregulated AKT1 expression in the Sch B treatment group, indicating a potentially important mechanism of action. ALB encodes albumin, the most abundant protein in human blood, which serves as an effective antioxidant and has been shown to provide organ protection in cerebral ischemia-reperfusion injury.[26] ALB reduces neuronal apoptosis following cerebral hemorrhage through the ERK/Nrf2/HO-1 signaling pathway.[27] In this study, the transcriptional level of albumin was upregulated, indicating enhanced antioxidant and anti-apoptotic effects. In a rat model of renal ischemia-reperfusion, activation of renin-angiotensin system (RAS) components, such as ACE, AT1R, AT2R, and Ang II, was significantly elevated in plasma. Treatment with ACE inhibitors alleviated renal pathological damage and partially restored renal function.[28] Our

study confirmed that ACE transcription levels increased during RIRI, whereas pretreatment with Sch B reduced ACE expression levels. CCL5 is a small chemokine involved in immune regulation and inflammatory responses. The role and expression of CCL5 during organ ischemia-reperfusion injury are controversial. In cardiac IRI, Vincent Braunersreuther et al[29] identified CCL5 as a detrimental factor that enhances cardiac inflammatory responses. Notably, the use of CCL5/RANTES antagonists reduced infarct size and serum troponin I levels. However, the study also noted that mice lacking the CCL5/RANTES receptor CCR5 did not exhibit myocardial salvage functions. A study exploring the effects of natural sphingolipid N,N-dimethylsphingosine (DMS) on alleviating renal injury suggested that DMS exerts its protective effects by increasing the expression of chemokines CXCL9, CCL5, and CXCL10, thereby recruiting Treg cells to inflammatory sites for anti-inflammatory action.[30] Our study indicated that CCL5 expression significantly decreased in the IR group, while its expression was restored in the Sch B treatment group. This suggests that Sch B may directly or indirectly modulate immune cells to mitigate inflammatory responses. However, the specific mechanisms involved require further investigation.

Sch B has been demonstrated to mitigate cisplatin-induced apoptosis in renal cells via the PI3K/AKT signalling pathway and the downstream cysteine asparaginase signalling pathway.[24] However, there have been no studies on the signaling pathways through which Sch B exerts its effects in RIRI. Based on transcriptomic and network pharmacological analyses, along with in vitro validation, we preliminarily identified the PI3K/AKT signaling pathway as a key mechanism through which Sch B exerts its protective effects. Furthermore, recent research has shown that many drugs can activate the PI3K/AKT pathway to protect against RIRI, such as gastrin,[31] curcumin,[32] and fibroblast growth factor 2.[33] Our study, for the first time, suggests that Sch B may exert organ-protective effects by activating the PI3K/AKT pathway, with potential key targets including AKT1, ALB, ACE, and CCL5.

The limitations of this study include: (i) only a simple experimental validation of the transcriptomic and network pharmacological analysis results was performed, without an in-depth exploration of the mechanisms involved; (ii) our research lacks support from clinical data. These limitations will guide our future work.

Conclusion

This study is the first to reveal the protective mechanisms of Sch B against RIRI from the perspectives of transcriptomics and network pharmacology. The results demonstrate that Sch B effectively reduces oxidative stress, inflammatory responses, and apoptosis, thereby significantly improving renal function. This effect is achieved by regulating key targets such as AKT1, ALB, ACE, and CCL5, and activating the PI3K/AKT signaling pathway. These findings provide crucial molecular evidence for the therapeutic potential of Sch B as a renal protective agent. They open the door for future research into its clinical applications, particularly in the development of targeted therapies for renal injury. Further studies, including preclinical and clinical trials, will be essential to confirm its efficacy and safety in humans, thus facilitating its progression toward clinical use.

Funding

This paper is supported by The Special Fund Project for Central Guiding Local Science and Technology Development (24ZYQA050).

Disclosure

The authors report no conflicts of interest in this work.

References

1. Shan Y, Chen D, Hu B, et al. Allicin ameliorates renal ischemia/reperfusion injury via inhibition of oxidative stress and inflammation in rats. *Biomed Pharmacother*. 2021;142:112077. doi:10.1016/j.biopha.2021.112077
2. Zhou L, Tang S, Li F, et al. Ceria nanoparticles prophylactic used for renal ischemia-reperfusion injury treatment by attenuating oxidative stress and inflammatory response. *Biomaterials*. 2022;287:121686. doi:10.1016/j.biomaterials.2022.121686
3. Lau A, Rahn JJ, Chappellaz M, et al. Dipeptidase-1 governs renal inflammation during ischemia reperfusion injury. *Sci Adv*. 2022;8:eabm0142.
4. Daemen MA, van 't Veer C, Denecker G, et al. Inhibition of apoptosis induced by ischemia-reperfusion prevents inflammation. *J Clin Invest*. 1999;104:541–549. doi:10.1172/JCI6974

5. Zhao H, Alam A, Soo AP, George AJT, Ma D. Ischemia-reperfusion injury reduces long term renal graft survival: mechanism and beyond. *EBioMedicine*. 2018;28:31–42. doi:10.1016/j.ebiom.2018.01.025
6. Luo W, Lin K, Hua J, et al. Schisandrin B attenuates diabetic cardiomyopathy by targeting MyD88 and Inhibiting MyD88-Dependent Inflammation. *Adv Sci*. 2022;9:e2202590.
7. Zhang Q, Liu J, Duan H, Li R, Peng W, Wu C. Activation of Nrf2/HO-1 signaling: an important molecular mechanism of herbal medicine in the treatment of atherosclerosis via the protection of vascular endothelial cells from oxidative stress. *J Adv Res*. 2021;34:43–63. doi:10.1016/j.jare.2021.06.023
8. Li WL, Xin HW, Yu AR, Wu XC. In vivo effect of Schisandrin B on cytochrome P450 enzyme activity. *Phytomedicine*. 2013;20:760–765. doi:10.1016/j.phymed.2013.02.005
9. Qin XL, Chen X, Zhong GP, et al. Effect of Tacrolimus on the pharmacokinetics of bioactive lignans of Wuzhi tablet (Schisandra sphenanthera extract) and the potential roles of CYP3A and P-gp. *Phytomedicine*. 2014;21:766–772. doi:10.1016/j.phymed.2013.12.006
10. Zhu W, Luo W, Han J, et al. Schisandrin B protects against LPS-induced inflammatory lung injury by targeting MyD88. *Phytomedicine*. 2023;108:154489. doi:10.1016/j.phymed.2022.154489
11. Chiu PY, Leung HY, Siu AH, Poon MK, Ko KM. Schisandrin B decreases the sensitivity of mitochondria to calcium ion-induced permeability transition and protects against ischemia-reperfusion injury in rat hearts. *Acta Pharmacol Sin*. 2007;28:1559–1565. doi:10.1111/j.1745-7254.2007.00614.x
12. Stoeckius M, Hafemeister C, Stephenson W, et al. Simultaneous epitope and transcriptome measurement in single cells. *Nat Methods*. 2017;14(9):865–868. doi:10.1038/nmeth.4380
13. Nogales C, Mamdouh ZM, List M, Kiel C, Casas AI, Schmidt H. Network pharmacology: curing causal mechanisms instead of treating symptoms. *Trends Pharmacol Sci*. 2022;43:136–150. doi:10.1016/j.tips.2021.11.004
14. Chu LK, Cao X, Wan L, et al. Autophagy of OTUD5 destabilizes GPX4 to confer ferroptosis-dependent kidney injury. *Nat Commun*. 2023;14:8393. doi:10.1038/s41467-023-44228-5
15. Xue JY, Liu GT, Wei HL, Pan Y. Antioxidant activity of two dibenzocyclooctene lignans on the aged and ischemic brain in rats. *Free Radic Biol Med*. 1992;12:127–135. doi:10.1016/0891-5849(92)90006-3
16. Cao JY, Wang B, Tang TT, et al. Exosomal miR-125b-5p deriving from mesenchymal stem cells promotes tubular repair by suppression of p53 in ischemic acute kidney injury. *Theranostics*. 2021;11:5248–5266. doi:10.7150/thno.54550
17. Carlström M, Guimaraes D, Boeder A, Schiffer TA. Dimethyl malonate preserves renal and mitochondrial functions following ischemia-reperfusion via inhibition of succinate dehydrogenase. *Redox Biol*. 2024;69:102984. doi:10.1016/j.redox.2023.102984
18. Hu S, Li Z, Shen D, et al. Exosome-eluting stents for vascular healing after ischaemic injury. *Nat Biomed Eng*. 2021;5:1174–1188. doi:10.1038/s41551-021-00705-0
19. Kar F, Hacioglu C, Senturk H, Donmez DB, Kanbak G, Uslu S. Curcumin and LOXblock-1 ameliorate ischemia-reperfusion induced inflammation and acute kidney injury by suppressing the semaphorin-plexin pathway. *Life Sci*. 2020;256:118016. doi:10.1016/j.lfs.2020.118016
20. Kar F, Hacioglu C, Senturk H, Donmez DB, Kanbak G. The role of oxidative stress, renal inflammation, and apoptosis in post ischemic reperfusion injury of kidney tissue: the protective effect of dose-dependent boric acid administration. *Biol Trace Elem Res*. 2020;195:150–158. doi:10.1007/s12011-019-01824-1
21. Zhang W, Sun Z, Meng F. Schisandrin B ameliorates myocardial ischemia/reperfusion injury through attenuation of endoplasmic reticulum stress-induced apoptosis. *Inflammation*. 2017;40:1903–1911. doi:10.1007/s10753-017-0631-4
22. Zhu N, Cai C, Zhou A, Zhao X, Xiang Y, Zeng C. Schisandrin B prevents hind limb from ischemia-reperfusion-induced oxidative stress and inflammation via MAPK/NF-κB pathways in rats. *Biomed Res Int*. 2017;2017:4237973. doi:10.1155/2017/4237973
23. Milliken AS, Nadtochiy SM, Brookes PS. Inhibiting succinate release worsens cardiac reperfusion injury by enhancing mitochondrial reactive oxygen species generation. *J Am Heart Assoc*. 2022;11:e026135.
24. Hu JN, Wang YM, Zhang H, et al. Schisandra B, a representative lignan from Schisandra chinensis, improves cisplatin-induced toxicity: an in vitro study. *Phytother Res*. 2023;37:658–671. doi:10.1002/ptr.7644
25. Lin HY, Chen Y, Chen YH, et al. Tubular mitochondrial AKT1 is activated during ischemia reperfusion injury and has a critical role in predisposition to chronic kidney disease. *Kidney Int*. 2021;99:870–884. doi:10.1016/j.kint.2020.10.038
26. Pinsky M, Roy U, Moshe S, Weissman Z, Kornitzer D. Human serum albumin facilitates heme-iron utilization by fungi. *mBio*. 2020;2020:11.
27. Belayev L, Saul I, Busto R, et al. Albumin treatment reduces neurological deficit and protects blood-brain barrier integrity after acute intracortical hematoma in the rat. *Stroke*. 2005;36:326–331. doi:10.1161/01.STR.0000152949.31366.3d
28. Krishan P, Sharma A, Singh M. Effect of angiotensin converting enzyme inhibitors on ischaemia-reperfusion-induced renal injury in rats. *Pharmacol Res*. 1998;37:23–29. doi:10.1006/phrs.1997.0259
29. Montecucco F, Braunersreuther V, Lenglet S, et al. CC chemokine CCL5 plays a central role impacting infarct size and post-infarction heart failure in mice. *Eur Heart J*. 2012;33:1964–1974.
30. Lai LW, Yong KC, Lien YH. Pharmacologic recruitment of regulatory T cells as a therapy for ischemic acute kidney injury. *Kidney Int*. 2012;81:983–992. doi:10.1038/ki.2011.412
31. Liu C, Chen K, Wang H, et al. Gastrin attenuates renal ischemia/reperfusion injury by a PI3K/Akt/Bad-mediated anti-apoptosis signaling. *Front Pharmacol*. 2020;11:540479. doi:10.3389/fphar.2020.540479
32. Shi HH, Chen LP, Wang CC, et al. Docosahexaenoic acid-acylated curcumin diester alleviates cisplatin-induced acute kidney injury by regulating the effect of gut microbiota on the lipopolysaccharide- and trimethylamine-N-oxide-mediated PI3K/Akt/NF-κB signaling pathway in mice. *Food Funct*. 2022;13:6103–6117. doi:10.1039/D1FO04178A
33. Tan X, Tao Q, Li G, et al. Fibroblast growth factor 2 attenuates renal ischemia-reperfusion injury via inhibition of endoplasmic reticulum stress. *Front Cell Dev Biol*. 2020;8:147. doi:10.3389/fcell.2020.00147